



ELSEVIER



Journal of Computational and Applied Mathematics III (IIII) III-III

JOURNAL OF
 COMPUTATIONAL AND
 APPLIED MATHEMATICS

www.elsevier.com/locate/cam

Kernel-based methods for inversion of the Radon transform on $SO(3)$ and their applications to texture analysis

K.G. van den Boogaart^a, R. Hielscher^b, J. Prestin^{c,*}, H. Schaeben^b

^a*Department of Mathematics and Computer Science, Ernst-Moritz-Arndt-University Greifswald, D-17489 Greifswald, Germany*

^b*Institute of Geology, Freiberg University of Mining and Technology, Bernhard-von-Cotta Straße 2, D-09596 Freiberg, Germany*

^c*Institute of Mathematics, University of Lübeck, Wallstraße 40, D-23560 Lübeck, Germany*

Abstract

Texture analysis is used here as short term for analysis of crystallographic preferred orientation. Its major mathematical objective is the determination of a reasonable orientation probability density function and corresponding crystallographic axes probability density functions from experimentally accessible diffracted radiation intensity data. Since the spherical axes probability density function is modelled by the one-dimensional Radon transform for $SO(3)$, the problem is its numerical inversion. To this end, the Radon transform is characterized as an isometry between appropriate Sobolev spaces. The mathematical foundations as well as first numerical results with zonal basis functions are presented.

© 2005 Published by Elsevier B.V.

1. Introduction

The analysis of crystallographic preferred orientations by means of orientation density functions and pole density functions is a widely used method in texture analysis (cf. [2,10]). On the other hand, the zonal basis function method (cf. [9]) or kriging method with covariance functions (cf. [17]) has already found its way into many fields of application. Utilizing the zonal basis function method to interpolate pole figure intensities and to reconstruct the orientation density function of a specimen we introduce a new method in addition to hitherto used harmonic method (cf. [2]), WIMV (cf. [10]), maximum entropy (cf. [13]), or component fit method (cf. [8]). The main advantage of the zonal basis function method is that it can deal with X-ray intensities that are measured for arbitrary arranged crystal and specimen directions. In particular, the method is not restricted to data that are measured in pole figure notation, i.e., for a few crystal directions and many specimen directions.

We consider a polycrystalline specimen that consists only of one type of crystals. To this type one can associate a certain point group $G \subseteq SO(3)$ characterizing its symmetries (cf. [15]). Furthermore, each crystal provides a canonical crystal coordinate system which is well defined up to actions of the point group G . Fixing a specimen coordinate system we define the orientation of a crystal to be the rotation $g \in SO(3)/G$ that realizes the basis transformation from the crystal coordinate system to the specimen coordinate system. Directions relative to the crystal coordinate system we

* Corresponding author.

E-mail addresses: gerald.boogaart@uni-greifswald.de (K.G. van den Boogaart), ralf.hielscher@geo.tu-freiberg.de (R. Hielscher), prestin@math.uni-luebeck.de (J. Prestin), schaeben@geo.tu-freiberg.de (H. Schaeben).

1 will call crystal directions and directions relative to the specimen coordinate system specimen directions. Hence, every
orientation of a crystal rotates crystal directions onto specimen directions.

3 The orientation density function (ODF) $f: \text{SO}(3)/G \rightarrow \mathbb{R}$ is defined as the relative frequency of orientations by
volume within a specimen, whereas the pole density function (PDF) $P: S^2/G \times S^2 \rightarrow \mathbb{R}$ is defined as the relative
5 frequency $P(h, r)$ of orientations $g \in \text{SO}(3)/G$ rotating the crystal direction $h \in S^2/G$ onto the specimen direction
 $r \in S^2$. The ODF f and the PDF P of a specimen are connected by the crystallographic X-ray transform on $\text{SO}(3)/G$.
7 Denote $G(h, r) = \{g \in \text{SO}(3)/G \mid r \in gh\}$ the set of all orientations $g \in \text{SO}(3)/G$ that maps a given crystal direction
 $h \in S^2/G$ onto a given specimen direction $r \in S^2$. With the help of the one-dimensional Radon transform on $\text{SO}(3)/G$,

$$\mathcal{R}: C(\text{SO}(3)/G) \rightarrow C(S^2/G \times S^2),$$

$$9 \quad \mathcal{R}f(h, r) := \int_{G(h,r)} f(g) \, dg$$

we define the crystallographic X-ray transform

$$\mathcal{X}: C(\text{SO}(3)/G) \rightarrow C(S^2/G \times S^2),$$

$$11 \quad \mathcal{X}f(h, r) := \frac{1}{2} (\mathcal{R}f(h, r) + \mathcal{R}f(-h, r)).$$

The fundamental result of Bunge (cf. [2, Section 4.2]) states that

$$13 \quad P(h, r) = \mathcal{X}f(h, r).$$

For a fixed crystal direction $h \in S^2/G$ the PDF $P(h, \cdot): S^2 \rightarrow \mathbb{R}$ is called pole figure. Conversely, fixing specimen
15 directions $r \in S^2$ we obtain inverse pole figures $P(\cdot, r)$ which allows to investigate the anisotropy of the specimen.

There are several experiments like X-ray, neutron, and synchrotron diffraction that allows to measure the PDF of a
17 specimen for a sequence of crystal and specimen directions. To such a list of PDF measurements $(P_i)_{i=1}^N$ with respect
to crystal and specimen directions $(h_i, r_i)_{i=1}^N$ we refer as to a set of X-ray intensities $(P_i, h_i, r_i)_{i=1}^N$. It is a central
19 problem in texture analysis to reconstruct the true PDF P and the true ODF f from a set of X-ray intensities. Since
both, ODF and PDF, are not uniquely determined by the data set we have to make additional assumptions to obtain
21 approximations \tilde{f} and \tilde{P} of the true density functions. It seems quite natural to ask for an ODF \tilde{f} and a PDF \tilde{P} that
fit best to the pole figure data and are sufficiently smooth. In order to specify these conditions we introduce in Section
23 2.3 Sobolev spaces $\mathcal{H}(\text{SO}(3))$ and $\mathcal{H}(S^2 \times S^2)$ on $\text{SO}(3)$ and $S^2 \times S^2$, respectively. Taking the Sobolev norm as a
measure of smoothness such functions \tilde{f} and \tilde{P} are given as the solution of the minimization problems

$$25 \quad \frac{1}{N} \sum_{i=1}^N (\mathcal{X}f(h_i, r_i) - P_i)^2 + \lambda \|f\|_{\mathcal{H}(\text{SO}(3))}^2 \rightarrow \min \quad (f \in \mathcal{H}(\text{SO}(3))) \quad (1.1)$$

and

$$27 \quad \frac{1}{N} \sum_{i=1}^N (P(h_i, r_i) - P_i)^2 + \lambda \|P\|_{\mathcal{H}(S^2 \times S^2)}^2 \rightarrow \min \quad (P \in \mathcal{H}(S^2 \times S^2)). \quad (1.2)$$

Here, the regularization parameter $\lambda > 0$ determines the balance between fitting to the given data set and smoothness
29 of the solution.

In Theorem 2.11 we present conditions which ensure that the Radon transform is an isometry between the Sobolev
31 spaces $\mathcal{H}(\text{SO}(3))$ and $\mathcal{H}(S^2 \times S^2)$. Moreover, in the Theorems 2.15 and 2.17 we characterize the Sobolev spaces
 $\mathcal{H}(\text{SO}(3))$ and $\mathcal{H}(S^2 \times S^2)$ which turn out to be reproducing kernel Hilbert spaces. In this case the solutions of the
33 minimization problems (1.1) and (1.2) can be identified as the solutions of corresponding systems of linear equations.
Thus, applying Sobolev norms as measures of smoothness of the ODF and its X-ray transform and Corollary 2.18 as
35 the major result of Section 2 leads to a novel numerical inversion of the Radon and the restricted X-ray transform by
approximation with zonal basis functions which is presented in Section 3. It is emphasized that these basis functions
37 are radial with respect to the fibres $\{gh_i = r_i \mid g \in \text{SO}(3)\}$. Hence, our ODF is constructed by a linear combination
of fibre ODFs. Let us note that the fibre-symmetric radial basis functions are very much related to the ridge functions

discussed by Donoho (cf. [4]). The Radon transform of the ridge functions as well as of the fibre-symmetric radial basis functions provides a system of well-localized functions in frequency and space.

In Section 2.5 we give an example of a zonal basis function which allows an explicit representation of the recalculated ODF and its X-ray transform. Furthermore, in Theorem 3.3 we prove an error estimate and finally we discuss some numerical results obtained with a *Matlab* implementation of the method.

2. The Radon transform on SO(3)

Throughout this paper three domains of integration S^2 , $\text{SO}(3)$ and $G[h, r] := \{g \in \text{SO}(3) \mid gh = r\}$ (cf. Section 2.2) appear frequently. These domains we assume to be equipped with its canonical Haar measure, normed to one.

2.1. Basis systems on S^2 and $\text{SO}(3)$

We start our considerations by introducing some notations and fundamental results concerning functions on S^2 and $\text{SO}(3)$ (cf. [12]). The starting point of all work on the sphere are the Legendre Polynomials \mathcal{P}_l of degree $l \in \mathbb{N}_0$ given by

$$\mathcal{P}_l(t) = \frac{1}{2^l l!} \frac{d^l}{dt^l} ((t^2 - 1)^l) \quad (t \in [-1, 1])$$

and the associated Legendre Polynomials \mathcal{P}_l^k , $l, k \in \mathbb{N}_0$ with $k \leq l$ given by

$$\mathcal{P}_l^k(t) = \left(\frac{(l-k)!}{(l+k)!} \right)^{1/2} (1-t^2)^{k/2} \frac{d^k}{dt^k} \mathcal{P}_l(t) \quad (t \in [-1, 1]).$$

In terms of the associated Legendre Polynomials we define an orthonormal basis of the space of spherical harmonics $\text{Harm}_l(S^2)$ of degree $l \in \mathbb{N}_0$ by

$$\mathcal{Y}_l^k(\theta, \rho) = \sqrt{2l+1} \mathcal{P}_l^{|k|}(\cos \theta) e^{ik\rho} \quad (k = -l, \dots, l).$$

In this formula (θ, ρ) are the polar coordinates of a point on the sphere S^2 . Since $L^2(S^2) = \text{clos}_{L^2}(\bigoplus_{l=0}^{\infty} \text{Harm}_l(S^2))$ the function system $(\mathcal{Y}_l^k)_{l \in \mathbb{N}_0, k=-l, \dots, l}$ provides an orthonormal basis of $L^2(S^2)$. Corresponding to this basis we define the Fourier coefficients of a function $f \in L^2(S^2)$ to be

$$\hat{f}(l, k) = \int_{S^2} f(\xi) \overline{\mathcal{Y}_l^k(\xi)} d\xi \quad (l \in \mathbb{N}_0, k = -l, \dots, l).$$

For the vector of functions $(\mathcal{Y}_l^{-l}, \dots, \mathcal{Y}_l^l)^t$ we will write just \mathcal{Y}_l . The well-known addition theorem can now be viewed as

$$(2l+1)\mathcal{P}_l(\xi^t \eta) = \mathcal{Y}_l(\xi)^t \overline{\mathcal{Y}_l(\eta)}. \quad (2.1)$$

There are different ways to introduce basis systems in $L^2(\text{SO}(3))$. The way we start with is based on representation theory. It is well known that for $l \in \mathbb{N}_0$ the translations

$$\begin{aligned} \mathcal{T}_l: \text{SO}(3) &\rightarrow \text{GL}(\text{Harm}_l(S^2)), \\ \mathcal{T}_l(g)f(\xi) &= f(g\xi) \end{aligned} \quad (2.2)$$

form a complete system of irreducible finite dimensional representations of the group $\text{SO}(3)$. Let $T_l = (T_l^{i,j})_{i,j=-l}^l$ be the matrix corresponding to the operators \mathcal{T}_l . Now the Peter-Weyl theorem and its conclusions (cf. [16, Sections 2.3.4 and 2.3.5]) states that for $i, j = -l, \dots, l$ the normalized matrix elements $\sqrt{2l+1} T_l^{i,j}$ with

$$T_l^{ij}(g) = \langle \mathcal{Y}_l^i(g \cdot), \mathcal{Y}_l^j(\cdot) \rangle_{L^2(S^2)} = \int_{S^2} \mathcal{Y}_l^i(g\xi) \overline{\mathcal{Y}_l^j(\xi)} d\xi \quad (g \in \text{SO}(3)) \quad (2.3)$$

1 define an orthonormal basis of $L^2(\text{SO}(3))$. The matrix elements $T_l^{i,j}$ are also called generalized spherical harmonics
of degree l (cf. [2, Section 11.1]). The definition of T_l can also be written as

$$3 \quad T_l(g)\mathcal{Y}_l(\xi) = \mathcal{Y}_l(g\xi) \quad (g \in \text{SO}(3), \xi \in S^2).$$

Let us look at the basis functions on $\text{SO}(3)$ from a different view. Denote S^3 the three-dimensional unit sphere
embedded in the space of quaternions \mathbb{H} . Then observing that $q, -q \in S^3 \subseteq \mathbb{H}$ define the same rotation $\mathbb{R}^3 \ni x \mapsto$
 $qx\bar{q}$ we see that S^3 is a two-fold covering of $\text{SO}(3)$. Since the Haar measure on $\text{SO}(3)$ is the induced measure of the
spherical measure on S^3 the space $L^2(\text{SO}(3))$ is isomorphic to $\{f \in L^2(S^3) \mid \forall q \in S^3 : f(-q) = f(q)\}$ and therefore
the direct sum of the spaces of spherical harmonics $\text{Harm}_{2l}(S^3)$ of even degree $2l$ (cf. [12]). In particular, for $l \geq 0$ the
normalized matrix entries $T_l^{i,j}, i, j = -l, \dots, l$ provide an orthonormal basis of $\text{Harm}_l(S^3)$. As a consequence we can
formulate the addition theorem for the generalized spherical harmonics (cf. [12, Theorem 2]).

11 **Theorem 2.1.** *Let T_l be defined as in Eq. (2.3). Then $\text{Tr } T_l(g) = \sum_{i=-l}^l T_l^{i,i}(g)$ depends only on the rotation angle
 $\omega(g)$ of g . In particular, it yields*

$$13 \quad \text{Tr } T_l(g) = \frac{\sin(((2l+1)/2)\omega(g))}{\sin(\frac{1}{2}\omega(g))} = \mathcal{U}_{2l}\left(\cos\left(\frac{\omega(g)}{2}\right)\right),$$

where \mathcal{U}_l denotes the Chebychev polynomial of second kind and degree l .

15 A function on $\text{SO}(3)$ depending only on the distance to some fixed rotation is called radial basis function. From
Theorem 2.1 we conclude that every square integrable radial basis function on $\text{SO}(3)$ has a Fourier expansion in terms
of Chebychev polynomials of even degree.

2.2. The Radon transform as an L^2 -operator

19 The Radon transform appears in many guises and different settings. A comprehensive introduction can be found in
Helgason [7]. The standard Radon transform on \mathbb{R}^2 maps each continuous function with compact support $f \in C_c(\mathbb{R}^2)$
onto its integrals along all straight lines. It was shown by Radon that knowing all these integrals one can reconstruct
 f . The orientation density function defined on the group of rotations $\text{SO}(3)$ plays the role of f in texture analysis.
23 The paths of integration are all one-dimensional great circles $G[h, r] = \{g \in \text{SO}(3) \mid gh = r\}$ parameterized by all
pairs $(h, r) \in S^2$ of crystal and specimen directions. Since the integral over $G[h, r]$ of a continuous function varies
continuously with respect to h and r we can define the one-dimensional Radon transform on $\text{SO}(3)$ as the operator

$$\begin{aligned} \tilde{\mathcal{R}}: C(\text{SO}(3)) &\rightarrow C(S^2 \times S^2), \\ (\tilde{\mathcal{R}}f)(h, r) &= \int_{G[h,r]} f(g) \, dg. \end{aligned}$$

27 The path of integration $G[h, r]$ can be identified with the set of quaternions

$$Q[h, r] = \{q(\theta) = \cos(\theta)q_1 + \sin(\theta)q_2 \mid \theta \in [0, \pi)\},$$

29 where q_1 and q_2 are two quaternions representing rotations mapping h onto r —first about the axis $h+r$ and second about
the axis $h \times r$. For a detailed presentation of the geometry of the spherical Radon transform, the reader is referred to
31 Meister and Schaabben [11]. In terms of quaternions, the definition of $\tilde{\mathcal{R}}$ rewrites as

$$\tilde{\mathcal{R}}f(h, r) = \frac{1}{\pi} \int_0^\pi f(q(\theta)) \, d\theta. \quad (2.4)$$

33 This integration formula has two important special cases. Let f be a radial symmetric ODF, i.e., $f(g)$ depends only
on the rotation angle $\omega(g^{-1}g_0)$ of $g^{-1}g_0$ for a fixed $g_0 \in \text{SO}(3)$. Then there is a function \tilde{f} such that for all $g \in \text{SO}(3)$
35 one has $f(g) = \tilde{f}(\cos(\omega(g^{-1}g_0)/2))$. In this case Eq. (2.4) becomes (cf. [14])

$$\tilde{\mathcal{R}}f(h, r) = \frac{1}{\pi} \int_0^\pi \tilde{f}(\cos(\theta) \cos(\angle(g_0h, r)/2)) \, d\theta \quad (h, r \in S^2).$$

Let f be a fibre symmetric ODF, i.e., there are crystal and specimen directions $h_0, r_0 \in S^2$ and a function \tilde{f} such that $f(g) = \tilde{f}(\langle gh_0, r \rangle_0)$. We can obtain an integration formula from Eq. (2.4) by determining $\langle gh_0, r_0 \rangle$ from $q(\theta)$. Fixing $h, r \in S^2$ we conclude from $\angle(qh_0\bar{q}, r) = \angle(h_0, \bar{q}r) = \angle h_0 h$ for all $q \in \mathbb{H}$ with $qh\bar{q} = r$ that $\{qh_0\bar{q} \mid q \in Q[h, r]\}$ perform a small circle around r with radius $\angle h_0 h$ (cf. [11]). Therefore, we can choose a parameterization $q(\theta)$, $\theta \in [-\pi, \pi)$ of $Q[h, r]$ such that the angle at r in the spherical triangle $r, r_0, qh_0\bar{q}$ equals θ . By spherical trigonometry we compute the distance

$$\langle qh_0\bar{q}, r_0 \rangle = \cos(\angle hh_0) \cos(\angle rr_0) + \sin(\angle hh_0) \sin(\angle rr_0) \cos(\theta).$$

Finally, we find the integration formula

$$\tilde{\mathcal{R}}f(h, r) = \frac{1}{\pi} \int_0^\pi \tilde{f}(\cos(\angle hh_0) \cos(\angle rr_0) + \sin(\angle hh_0) \sin(\angle rr_0) \cos(\theta)) d\theta. \quad (2.5)$$

The next lemma on the Radon transform of the generalized spherical harmonics $T_l^{i,j}$ seems to be a well-known result (cf. [2, Section 11.5.2]). However, we were not able to locate a complete proof of it. Therefore, we show

Lemma 2.2. *Let $l \in \mathbb{N}_0$ and $i, j \in -l, \dots, l$. The Radon transform of $T_l^{i,j}$ is given by*

$$\tilde{\mathcal{R}}T_l^{i,j}(h, r) = \frac{1}{2l+1} \mathcal{Y}_l^i(r) \overline{\mathcal{Y}_l^j(h)} \quad (h, r \in S^2).$$

Proof. From Eq. (2.3) we obtain for arbitrary $l \geq 0$, $-l \leq i, j \leq l$

$$\begin{aligned} \tilde{\mathcal{R}}T_l^{i,j}(h, r) &= \int_{G[h,r]} T_l^{i,j}(g) dg \\ &= \int_{G[h,r]} \int_{S^2} \mathcal{Y}_l^i(gy) \overline{\mathcal{Y}_l^j(y)} dy dg \\ &= \int_{S^2} \overline{\mathcal{Y}_l^j(y)} \int_{G[h,r]} \mathcal{Y}_l^i(gy) dg dy. \end{aligned} \quad (2.6)$$

Since for every $y, h, r \in S^2$ we have $\{gy \mid g \in G[h, r]\} = \{x \in S^2 \mid \langle x, r \rangle = \langle h, y \rangle\}$ the inner integral rewrites as

$$\begin{aligned} \int_{G[h,r]} \mathcal{Y}_l^i(gy) dg &= \frac{1}{2\pi\sqrt{1 - \langle h, y \rangle^2}} \int_{\{x \in S^2 \mid \langle x, r \rangle = \langle h, y \rangle\}} \mathcal{Y}_l^i(x) dx dy \\ &= \mathcal{P}_l(\langle h, y \rangle) \mathcal{Y}_l^i(r). \end{aligned}$$

Here, we have applied the spherical mean value theorem on harmonic functions (cf. [5, equation 3.6.15]). Together with Eq. (2.6) we obtain

$$\tilde{\mathcal{R}}T_l^{i,j}(h, r) = \int_{S^2} \overline{\mathcal{Y}_l^j(y)} \mathcal{P}_l(\langle h, y \rangle) \mathcal{Y}_l^i(r) dy = \frac{1}{2l+1} \mathcal{Y}_l^i(r) \overline{\mathcal{Y}_l^j(h)}.$$

The last equality is due to the fact that $(2l+1)\mathcal{P}_l$ is the reproducing kernel of $\text{Harm}_l(S^2)$ (cf. [5, Lemma 3.1.4]). \square

Remark 2.3. Eq. (2.6) from Lemma 2.2 may be written as

$$\tilde{\mathcal{R}}T_l(h, r) = \frac{1}{2l+1} \mathcal{Y}_l(r) \overline{\mathcal{Y}_l(h)^t} \quad (h, r \in S^2).$$

An application to $\text{Tr } T_l$ gives

$$(\tilde{\mathcal{R}} \text{Tr } T_l)(h, r) = \frac{1}{2l+1} \sum_{i=-l}^l \mathcal{Y}_l^i(r) \overline{\mathcal{Y}_l^i(h)} = \mathcal{P}_l(\langle h, r \rangle).$$

Lemma 2.2 states in particular that $\tilde{\mathcal{R}}$ defines a $\|\cdot\|_{L^2(\text{SO}(3))} \rightarrow \|\cdot\|_{L^2(S^2 \times S^2)}$ bounded operator on a dense subset of $L^2(\text{SO}(3))$. Therefore, the following definition is valid.

1 **Definition 2.4.** The unique extension of the operator

$$\begin{aligned} \tilde{\mathcal{R}}: C(\text{SO}(3)) &\rightarrow C(S^2 \times S^2), \\ (\tilde{\mathcal{R}}f)(h, r) &= \int_{G[h,r]} f(g) \, dg \end{aligned}$$

3 to a bounded operator $\mathcal{R}: L^2(\text{SO}(3)) \rightarrow L^2(S^2 \times S^2)$ is called one-dimensional Radon transform on $\text{SO}(3)$.

We define also an averaged version of the Radon transform, known as crystallographic X-ray transform.

5 **Definition 2.5.** The operator

$$\begin{aligned} \mathcal{X}: L^2(\text{SO}(3)) &\rightarrow L^2(S^2 \times S^2), \\ (\mathcal{X}f)(h, r) &= \frac{1}{2}(\mathcal{R}f(h, r) + \mathcal{R}f(-h, r)) \end{aligned}$$

7 is called crystallographic X-ray transform.

The crystallographic X-ray transform provides the connection of the ODF f and the PDF P of a specimen (cf. [2, Section 4.2, 10, Section 9.2]), i.e., we have $\mathcal{X}f = P$.

11 From Lemma 2.2 we conclude that the Radon transform as well as the crystallographic X-ray transform has the following singular value decomposition.

13 **Corollary 2.6.** Let $l \in \mathbb{N}_0$ and \mathcal{Y}_l, T_l be defined as in Section 2.1. Then the Radon transform provides the singular value decomposition $(\sqrt{2l+1}T_l^{ij}, \mathcal{Y}_l^i \mathcal{Y}_l^j, 1/\sqrt{(2l+1)})$.

In particular, the X-ray transform has the singular value decomposition

$$15 \quad \mathcal{X}\sqrt{2l+1}T_l^{i,j}(h, r) = \begin{cases} \frac{1}{\sqrt{2l+1}} \mathcal{Y}_l^i(r) \overline{\mathcal{Y}_l^j(h)} & \text{if } l \text{ is even,} \\ 0 & \text{if } l \text{ is odd.} \end{cases}$$

17 **Remark 2.7.** The singular value decomposition of \mathcal{X} immediately shows that \mathcal{X} has a nonempty kernel spanned by the odd generalized spherical harmonics and therefore is not invertible. Furthermore, we can characterize the image of $L^2(\text{SO}(3))$ to be

$$19 \quad \mathcal{X}L^2(\text{SO}(3)) = \left\{ P(h, r) = \sum_{l \in 2\mathbb{N}_0} \sum_{i,j=-l}^l c_l^{i,j} \mathcal{Y}_l^i(r) \overline{\mathcal{Y}_l^j(h)} \mid \sum_{l \in 2\mathbb{N}_0} \sum_{i,j=-l}^l (2l+1)(c_l^{i,j})^2 < \infty \right\}.$$

2.3. The Radon transform as an isometry between Sobolev spaces

21 So far we have defined the Radon transform on $C(\text{SO}(3))$ and $L^2(\text{SO}(3))$. However, in order to characterize the Radon transform as an isometry which we can invert later on we have to deal with Sobolev spaces on $\text{SO}(3)$ and $S^2 \times S^2$. Our constructions are based on Sobolev spaces defined on the two-dimensional sphere S^2 . For more details and further reading we refer to Cheney and Light [3, Section 32] and Freeden et al. [5, Section 5.1].

25 **Definition 2.8.** Let $A = (A_l)_{l=0}^{\infty}$ be a nonnegative sequence. Denote $\aleph(A)$ the set of all indices of nonzero elements of a sequence $A = (A_l)$ in \mathbb{R} . The completion of the set of all functions $f \in L^2(\text{SO}(3))$ with

$$27 \quad f(g) = \sum_{l \in \aleph(A)} \sum_{i,j=-l}^l \sqrt{2l+1} \hat{f}(l, i, j) T_l^{i,j}(g)$$

1 satisfying $\sum_{l \in \mathfrak{N}(A)} \sum_{i,j=-l}^l A_l^2 |\hat{f}(l, i, j)|^2 < \infty$ with respect to the inner product

$$\langle f, g \rangle_{\mathcal{H}(A, \text{SO}(3))} = \sum_{l=0}^{\infty} \sum_{i,j=-l}^l A_l^2 \hat{f}(l, i, j) \overline{\hat{g}(l, i, j)}$$

3 is called Sobolev space $\mathcal{H}(A_l, \text{SO}(3))$. Here, $\hat{f}(l, i, j)$ denote the Fourier coefficients of f with respect to the L^2 -basis $(\sqrt{2l+1}T_l^{i,j})$.

5 Now we are going to define Sobolev spaces on $S^2 \times S^2$ which are suitable for the PDF interpolation problem. As we have mentioned in Remark 2.7, the PDF of a specimen has a Fourier expansion of the form

$$7 \quad P(h, r) = \sum_{l \in \mathbb{N}_0} \sum_{i,j=-l}^l \hat{P}(l, i, j) \mathcal{Y}_l^i(r) \overline{\mathcal{Y}_l^j(h)} \quad (r, h \in S^2).$$

Hence, we define a class of Sobolev spaces on $S^2 \times S^2$ of functions that have this particular Fourier expansion.

9 **Definition 2.9.** Let $B = (B_l)_{l=0}^{\infty}$ be a nonnegative sequence. The Sobolev space $\mathcal{H}(B_l, S^2 \times S^2)$ is defined as the completion of the set of all functions

$$11 \quad P(h, r) = \sum_{l \in \mathfrak{N}(B)} \sum_{i,j=-l}^l \hat{P}(l, i, j) \mathcal{Y}_l^i(r) \overline{\mathcal{Y}_l^j(h)} \quad (h, r \in S^2)$$

satisfying $\sum_{l \in \mathfrak{N}(B)} \sum_{i,j=-l}^l B_l^2 |\hat{P}(l, i, j)|^2 < \infty$ with respect to the inner product

$$13 \quad \langle P, Q \rangle_{\mathcal{H}(B_l, S^2 \times S^2)} = \sum_{l=0}^{\infty} \sum_{i,j=-l}^l B_l^2 \hat{P}(l, i, j) \overline{\hat{Q}(l, i, j)}.$$

Here $\hat{P}(l, i, j)$ denote the Fourier coefficients of P with respect to the L^2 -basis $(\mathcal{Y}_l^i \overline{\mathcal{Y}_l^j})$, $l=0, 1, 2, \dots, i, j=-l, \dots, l$.

15 **Remark 2.10.** It is a direct consequence of Definitions 2.8 and 2.9 that the sequences $(((\sqrt{2l+1})/A_l)T_l^{i,j})$ with $l \in \mathfrak{N}(A)$, $i, j = -l, \dots, l$ and $(B_l^{-1} \mathcal{Y}_l^i \overline{\mathcal{Y}_l^j})$ with $l \in \mathfrak{N}(B)$, $i, j = -l, \dots, l$ define orthonormal bases of the Sobolev spaces $\mathcal{H}(A_l, \text{SO}(3))$ and $\mathcal{H}(B_l, S^2 \times S^2)$.

19 For a suitable choice of the coefficients (A_l) and (B_l) we can extend the Radon transform to an isometry between the corresponding Sobolev spaces.

21 **Theorem 2.11.** Let $A = (A_l)$ be a nonnegative sequence and $B_l = \sqrt{2l+1}A_l$. Then the unique extension of the Radon transform

$$\mathcal{R}T_l^{i,j}(h, r) = \frac{1}{\sqrt{2l+1}} \mathcal{Y}_l^i(r) \overline{\mathcal{Y}_l^j(h)} \quad (l \in \mathbb{N}_0, i, j = -l, \dots, l)$$

23 to a bounded operator $\mathcal{R}: \mathcal{H}(A_l, \text{SO}(3)) \rightarrow \mathcal{H}(B_l, S^2 \times S^2)$ is an isometry.

25 **Proof.** We have only to show that \mathcal{R} preserves the inner product for all basis functions $(((\sqrt{2l+1})/A_l)T_l^{i,j})$ with $l \in \mathfrak{N}(A)$, $i, j = -l, \dots, l$ of $\mathcal{H}(A_l, \text{SO}(3))$. For $l, k \in \mathfrak{N}(A)$, $i, j = -l, \dots, l$ and $m, n = -k, \dots, k$ we calculate

$$\begin{aligned} \left\langle \mathcal{R} \frac{\sqrt{2l+1}}{A_l} T_l^{i,j}, \mathcal{R} \frac{\sqrt{2k+1}}{A_k} T_k^{m,n} \right\rangle_{\mathcal{H}(B_l, S^2 \times S^2)} &= \left\langle \frac{1}{\sqrt{2l+1}A_l} \mathcal{Y}_l^i \overline{\mathcal{Y}_l^j}, \frac{1}{\sqrt{2k+1}A_k} \mathcal{Y}_k^m \overline{\mathcal{Y}_k^n} \right\rangle_{\mathcal{H}(B_l, S^2 \times S^2)} \\ &= \left\langle \frac{1}{B_l} \mathcal{Y}_l^i \overline{\mathcal{Y}_l^j}, \frac{1}{B_k} \mathcal{Y}_k^m \overline{\mathcal{Y}_k^n} \right\rangle_{\mathcal{H}(B_l, S^2 \times S^2)} = \delta_{l,k} \delta_{i,m} \delta_{j,n}. \quad \square \end{aligned}$$

1 **Remark 2.12.** Let $\mathcal{H}(A_l, \text{SO}(3))$ and $\mathcal{H}(B_l, S^2 \times S^2)$ be as in Theorem 2.11 and $A_l = B_l = 0$ for l odd. Then the
 2 extension of the crystallographic X-ray transform \mathcal{X} to $\mathcal{H}(A_l, \text{SO}(3))$ provides an isometry onto $\mathcal{H}(B_l, S^2 \times S^2)$.
 3 Hence, \mathcal{X}^{-1} exists.

2.4. The Radon transform as an operator in reproducing kernel Hilbert spaces

5 Reproducing kernel Hilbert spaces turn out to be a basic tool for solving approximation problems. We present here
 6 only the most basic facts. For a more detailed representation, see for example, Freeden et al. [5, Section 5.2].

7 **Definition 2.13.** A Hilbert space $(\mathcal{H}, \langle \cdot, \cdot \rangle_{\mathcal{H}})$ is called a reproducing kernel Hilbert space if its elements $f \in \mathcal{H}$ are
 8 functions on a set Ω and for each $x \in \Omega$ the evaluation functional $f \mapsto f(x)$ is continuous.

9 Let \mathcal{H} be a reproducing kernel Hilbert space. The Riesz representation theorem implies that there is a well-defined
 10 function $K: \Omega \times \Omega \rightarrow \mathbb{R}$ such that for all $f \in \mathcal{H}$ and $x \in \Omega$ we have

$$11 \quad f(x) = \langle f, K(x, \cdot) \rangle_{\mathcal{H}}.$$

12 The function K is called reproducing kernel of \mathcal{H} . Since $K(x, y) = \langle K(x, \cdot), K(y, \cdot) \rangle_{\mathcal{H}} = K(y, x)$ each reproducing
 13 kernel is a symmetric function. Let $X = \{x_i\}_{i=1}^N$ be a set of N distinct points in Ω and $c = (c_i)_{i=1}^N$ some sequence in \mathbb{R} .
 14 Then the nonnegativity of the norm implies

$$15 \quad \sum_{i,j=1}^N c_i c_j K(x_i, x_j) = \left\langle \sum_{i=1}^N c_i K(x_i, \cdot), \sum_{i=1}^N c_i K(x_i, \cdot) \right\rangle_{\mathcal{H}} \geq 0. \quad (2.7)$$

16 This property of reproducing kernels is called positive definiteness. From Eq. (2.7) it follows in particular that the
 17 matrix $(K(x_i, x_j))_{i,j=1}^N$ is nonnegative definite.

We will also need the following lemma concerning isometries between reproducing kernel Hilbert spaces.

19 **Lemma 2.14.** Let $\mathcal{H}_1, \mathcal{H}_2$ be two reproducing kernel Hilbert spaces with domains Ω_1 and Ω_2 , respectively, and
 20 $A: \mathcal{H}_1 \rightarrow \mathcal{H}_2$ an isometry. Then the reproducing kernels K_1 and K_2 fulfill the equation

$$21 \quad AAK_1 = K_2,$$

where AAK_1 denotes the function on $\Omega_2 \times \Omega_2$ we obtained applying A to both arguments of K_1 .

23 **Proof.** Let $f \in \mathcal{H}_1$ and $\omega_2 \in \Omega_2$. Then $A_{\omega_2}: f \mapsto Af(\omega_2)$ defines a linear functional on \mathcal{H}_1 and we obtain

$$Af(\omega_2) = \langle f, A_{\omega_2} K_1 \rangle_{\mathcal{H}_1} = \langle Af, AA_{\omega_2} K_1 \rangle_{\mathcal{H}_2} = \langle Af, (AAK_1)(\omega_2, \cdot) \rangle_{\mathcal{H}_2}.$$

25 Hence, AAK_1 is the reproducing kernel of \mathcal{H}_2 . \square

26 The next theorem characterizes all Sobolev spaces on $\text{SO}(3)$ which are reproducing kernel Hilbert spaces. An
 27 analogous result for S^2 was proved by Freeden et al. [5, Lemma 5.2.2].

28 **Theorem 2.15.** Let $A = (A_l)_{l=0}^{\infty}$ be a nonnegative sequence. The Sobolev space $\mathcal{H}(A_l, \text{SO}(3))$ is a reproducing kernel
 29 Hilbert space, if and only if

$$30 \quad \sum_{l \in \mathbb{N}(A)} \frac{(2l+1)^2}{A_l^2} < \infty. \quad (2.8)$$

31 Furthermore, its reproducing kernel is given by the radial basis function

$$K_{\text{SO}(3)}(g_1, g_2) = \sum_{l \in \mathbb{N}(A)} \frac{2l+1}{A_l^2} \text{Tr } T_l(g_1^{-1} g_2).$$

- 1 **Proof.** Let $A = (A_l)$ be a nonnegative sequence satisfying inequality (2.8). According to Definition 2.13 we have to
 3 show that the evaluation functionals are bounded. Applying the Cauchy–Schwarz inequality to the Fourier expansion
 of an arbitrary function $f \in \mathcal{H}(A_l, \text{SO}(3))$ we obtain

$$\begin{aligned} |f(g)|^2 &= \left| \sum_{l \in \mathfrak{N}(A)} \sum_{i,j=-l}^l \sqrt{2l+1} \hat{f}(l, i, j) T_l^{i,j}(g) \right|^2 \\ &= \left| \sum_{l \in \mathfrak{N}(A)} \sum_{i,j=-l}^l A_l \hat{f}(l, i, j) \frac{\sqrt{2l+1}}{A_l} T_l^{i,j}(g) \right|^2 \\ &\leq \left(\sum_{l \in \mathfrak{N}(A)} \sum_{i,j=-l}^l A_l^2 |\hat{f}(l, i, j)|^2 \right) \left(\sum_{l \in \mathfrak{N}(A)} \frac{2l+1}{A_l^2} \sum_{i,j=-l}^l |T_l^{i,j}(g)|^2 \right). \end{aligned} \quad (2.9)$$

- 5 Using the definition (2.3) and Parseval’s relation the last sum reduces to

$$\sum_{i,j=-l}^l |T_l^{i,j}(g)|^2 = \sum_{i,j=-l}^l |\langle \mathcal{Y}_l^i, \mathcal{Y}_l^j(g \cdot) \rangle_{L^2(S^2)}|^2 = \sum_{j=-l}^l \|\mathcal{Y}_l^j(g \cdot)\|_{L^2(S^2)}^2 = 2l+1.$$

- 7 Since the first sum in (2.9) is the Sobolev norm of f we obtain the final estimate

$$|f(g)|^2 \leq \left(\sum_{l \in \mathfrak{N}(A)} \frac{(2l+1)^2}{A_l^2} \right) \|f\|_{\mathcal{H}(A_l, \text{SO}(3))}^2.$$

- 9 Hence, $\mathcal{H}(A_l, \text{SO}(3))$ is a reproducing kernel Hilbert space. Moreover, it follows from the fact that the Cauchy–Schwarz
 inequality is strict that condition (2.8) is necessary for $\mathcal{H}(A_l, \text{SO}(3))$ to be a reproducing kernel Hilbert space.

- 11 Since $\text{Tr } T_l \leq \text{Tr } T_l(\text{Id}) = 2l+1$ the function

$$K_{\text{SO}(3)}(g_1, g_2) = \sum_{l \in \mathfrak{N}(A)} \frac{2l+1}{A_l^2} \text{Tr } T_l(g_1^{-1} g_2)$$

- 13 is well defined for all sequences (A_l) satisfying (2.8). In order to show that $K_{\text{SO}(3)}$ is a reproducing kernel of
 $\mathcal{H}(A_l, \text{SO}(3))$ we verify for every $f(g) = T_k^{m,n}(g)$ with $k \in \mathfrak{N}(A)$ and $m, n = -k, \dots, k$ that

$$\begin{aligned} \langle f, K_{\text{SO}(3)}(g, \cdot) \rangle_{\mathcal{H}(A_l, \text{SO}(3))} &= \left\langle T_k^{m,n}, \sum_{l \in \mathfrak{N}(A)} \frac{2l+1}{A_l^2} \text{Tr } T_l(g)^t T_l \right\rangle_{\mathcal{H}(A_l, \text{SO}(3))} \\ &= \sum_{l \in \mathfrak{N}(A)} \sum_{i,j=-l}^l \frac{2l+1}{A_l^2} T_l^{i,j}(g) \langle T_k^{m,n}, T_l^{i,j} \rangle_{\mathcal{H}(A_l, \text{SO}(3))} \\ &= T_l^{m,n}(g). \end{aligned}$$

15

Hence, $K_{\text{SO}(3)}$ possesses the reproducing property on a dense subset of $\mathcal{H}(A_l, \text{SO}(3))$ and therefore on the whole
 17 Sobolev space. \square

- Remark 2.16.** Let $a = (a_l)_{l=0}^{\infty}$ be a nonnegative sequence, $A_l = \sqrt{(2l+1)/a_l}$ for $l \in \mathfrak{N}(a)$ and $A_l = 0$ otherwise.
 19 Then Theorem 2.15 implies that

$$\sum_{l \in \mathfrak{N}(a)} (2l+1)a_l < \infty$$

1 is equivalent to the condition that $\mathcal{H}(A_l, \text{SO}(3))$ is a reproducing kernel Hilbert space with the reproducing kernel

$$K_{\text{SO}(3)}(g_1, g_2) = \sum_{l \in \mathfrak{N}(a)} a_l \text{Tr } T_l(g_1^{-1} g_2).$$

3 In particular, this implies that $K_{\text{SO}(3)}$ is positive definite.

5 Analogously to Theorem 2.15 we characterize the reproducing kernel Hilbert spaces on $S^2 \times S^2$ which correspond to the Sobolev spaces $\mathcal{H}(B_l, S^2 \times S^2)$.

7 **Theorem 2.17.** *Let $B = (B_l)_{l=0}^{\infty}$ be a nonnegative sequence. The Sobolev space $\mathcal{H}(B_l, S^2 \times S^2)$ is a reproducing kernel Hilbert space, if and only if*

$$\sum_{l \in \mathfrak{N}(B)} \frac{(2l+1)^2}{B_l^2} < \infty. \quad (2.10)$$

9 Furthermore, its reproducing kernel is given by

$$K_{S^2 \times S^2}(h_1, r_1; h_2, r_2) = \sum_{l \in \mathfrak{N}(B)} \frac{(2l+1)^2}{B_l^2} \mathcal{P}_l(h_1 \cdot h_2) \mathcal{P}_l(r_1 \cdot r_2).$$

11 **Proof.** The proof follows the same ideas as the proof of Theorem 2.15. In order to show that the evaluation functionals are bounded we apply the Cauchy–Schwarz inequality and the addition Theorem 2.1 to the Fourier expansion of an
13 arbitrary function $P \in \mathcal{H}(B_l, S^2 \times S^2)$ and obtain

$$\begin{aligned} |P(h, r)|^2 &= \left| \sum_{l \in \mathfrak{N}(B)} \sum_{i, j=-l}^l \hat{P}(l, i, j) \mathcal{Y}_l^i(r) \overline{\mathcal{Y}_l^j(h)} \right|^2 \\ &= \left| \sum_{l \in \mathfrak{N}(B)} \sum_{i, j=-l}^l B_l \hat{P}(l, i, j) B_l^{-1} \mathcal{Y}_l^i(r) \overline{\mathcal{Y}_l^j(h)} \right|^2 \\ &\leq \left(\sum_{l \in \mathfrak{N}(B)} \sum_{i, j=-l}^l B_l^2 |\hat{P}(l, i, j)|^2 \right) \left(\sum_{l=0}^{\infty} \sum_{i, j=-l}^l B_l^{-2} |\mathcal{Y}_l^i(r)|^2 |\mathcal{Y}_l^j(h)|^2 \right) \\ &\leq \left(\sum_{l \in \mathfrak{N}(B)} \frac{(2l+1)^2}{B_l^2} \right) \|P\|_{\mathcal{H}(B_l, S^2 \times S^2)}^2. \end{aligned}$$

15 Hence, $\mathcal{H}(B_l, S^2 \times S^2)$ is a reproducing kernel Hilbert space. The necessity of the constraint (2.10) results from the strictness of the Cauchy–Schwarz inequality.

17 It is straightforward to see that for every sequence (B_l) satisfying (2.10) the function

$$K_{S^2 \times S^2}(h_1, r_1; h_2, r_2) = \sum_{l \in \mathfrak{N}(B)} \frac{(2l+1)^2}{B_l^2} \mathcal{P}_l(h_1 \cdot h_2) \mathcal{P}_l(r_1 \cdot r_2)$$

19 is well defined. In order to prove that $K_{S^2 \times S^2}$ is the reproducing kernel we verify for every $P(h, r) = \mathcal{Y}_l^i(r) \overline{\mathcal{Y}_l^j(h)}$ with $l \in \mathfrak{N}(B)$ and $i, j \in -l, \dots, l$ that

$$\begin{aligned} \langle P, K_{S^2 \times S^2}(h, r; \cdot) \rangle_{\mathcal{H}(B_l, S^2 \times S^2)} &= \left\langle \mathcal{Y}_l^i \overline{\mathcal{Y}_l^j}, \sum_{k \in \mathfrak{N}(B)} \sum_{m, n=-k}^k B_k^{-2} \mathcal{Y}_k^n(r) \overline{\mathcal{Y}_k^m(h)} \mathcal{Y}_k^m \right\rangle_{\mathcal{H}(B_l, S^2 \times S^2)} \\ &= \mathcal{Y}_l^i(r) \overline{\mathcal{Y}_l^j(h)}. \quad \square \end{aligned}$$

21

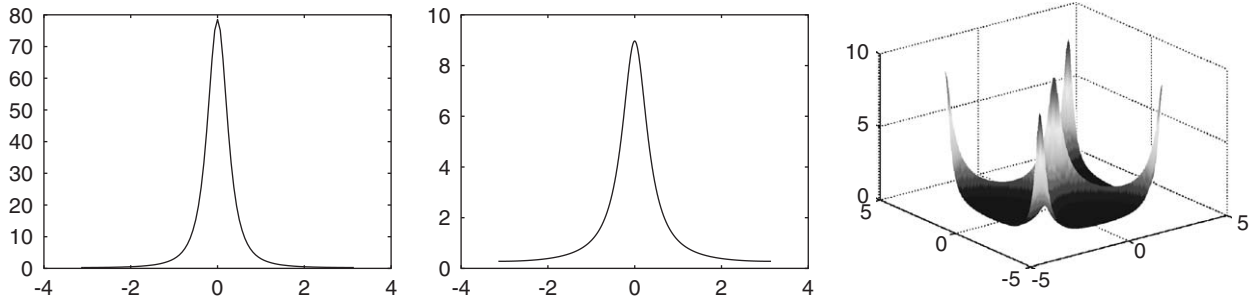


Fig. 1. The squared singularity kernel for $\kappa = 0.7$. From the left: K , $\mathcal{R}K$ and $\mathcal{R}\mathcal{R}K$.

1 Combining the results of the previous two sections we obtain

Corollary 2.18. Let $A = (A_l)_{l=0}^{\infty}$ be some nonnegative sequence such that $\mathcal{H}(A_l, \text{SO}(3))$ defines a reproducing kernel Hilbert space and $B_l = \sqrt{2l+1}A_l$. Then $\mathcal{H}(B_l, S^2 \times S^2)$ defines a reproducing kernel Hilbert space on $S^2 \times S^2$.

3 Moreover, the restriction of the Radon transform on $\mathcal{H}(A_l, \text{SO}(3))$ defines an isometry onto $\mathcal{H}(B_l, S^2 \times S^2)$. In
5 particular, the reproducing kernels satisfy the equality

$$K_{S^2 \times S^2} = \mathcal{R}\mathcal{R}K_{\text{SO}(3)}. \quad (2.11)$$

7 **Proof.** The space $\mathcal{H}(B_l, S^2 \times S^2)$ defines a reproducing kernel Hilbert space which follows as a direct consequence
of Theorems 2.15 and 2.17. Theorem 2.11 states that $\mathcal{R}: \mathcal{H}(A_l, \text{SO}(3)) \rightarrow \mathcal{H}(B_l, S^2 \times S^2)$ is an isometry. Eq. (2.11)
9 was shown in Lemma 2.14 for arbitrary isometries between reproducing kernel Hilbert spaces. \square

2.5. The squared singularity kernel

11 For the numerical work we are interested in kernel functions K on $\text{SO}(3)$ with closed formulas for $\mathcal{R}K$ and $\mathcal{R}\mathcal{R}K$.
However, it turns out that it is difficult to find an explicit formula for the double Radon transform $\mathcal{R}\mathcal{R}K$ of a given
13 kernel K on $\text{SO}(3)$. Since for solving the ODF to PDF inversion problem we will need explicitly only $\mathcal{R}K$ and $\mathcal{R}\mathcal{R}K$
we can start with a simple function for $\mathcal{R}K$. Let us consider a kernel function defined as the square of the well-known
15 singularity kernel (cf. [5, Section 5.6]). This kernel we call squared singularity kernel which is given for $\kappa \in (0, 1)$ by

$$\mathcal{R}K(h, r, g) = \left(\ln \frac{1+\kappa}{1-\kappa} \right)^{-1} \frac{2\kappa}{1 - 2\kappa \langle gh, r \rangle + \kappa^2} \quad (h, r \in S^2, g \in \text{SO}(3)).$$

17 The parameter κ determines the concentration of the kernel. Note that we do not have an explicit formula for $K: \text{SO}(3) \times$
 $\text{SO}(3) \rightarrow \mathbb{R}$. However, by the isomorphism \mathcal{R} the kernel K is uniquely defined. In Fig. 1 is plotted the squared singularity
19 kernel K as a function of $\omega = \omega(g_1^{-1}g_2)$, the Radon transformed kernel $\mathcal{R}K(\omega)$ as a function of $\omega = \langle gh, r \rangle$ and the
double Radon transformed kernel $\mathcal{R}\mathcal{R}K(\omega_h, \omega_r)$ as a function of $\omega_h = \angle h_1 h_2, \omega_r = \angle r_1 r_2$.

21 Next we show that this kernel serves as a reproducing kernel.

Theorem 2.19. The Legendre coefficients a_l of the squared singularity kernel $\mathcal{R}K$ satisfy the inequality

$$23 \quad 0 < a_l \leq \kappa^{l-1} \ln \frac{1+\kappa}{1-\kappa} \quad \text{for } l = 0, 1, 2, \dots$$

In particular, K is the reproducing kernel of $\mathcal{H}(\sqrt{(2l+1)}/a_l, \text{SO}(3))$.

1 **Proof.** For abbreviation let $\omega = \langle gh, r \rangle$ and $Q(\omega) = (1 - 2\kappa\omega + \kappa^2)^{-1}$. In order to show the positivity we use the Rodriguez's formula for Legendre polynomials to obtain for $l \geq 0$

$$\begin{aligned} a_l &= \int_{S^2} \mathcal{R}K(g, h, r) \mathcal{P}_l(gh \cdot r) \, dr = \int_{-1}^1 Q(\omega) \mathcal{P}_l(\omega) \, d\omega \\ &= \frac{1}{2^l l!} \int_{-1}^1 Q^{(l)}(\omega) (1 - \omega^2)^l \, d\omega \\ &= \frac{1}{2^l l!} \int_{-1}^1 \frac{2^l l! \kappa^l}{(1 + \kappa^2 - 2\kappa\omega)^{l+1}} (1 - \omega^2)^l \, d\omega > 0. \end{aligned}$$

Using $0 \leq 1 - \omega^2 \leq 1 + \kappa^2 - 2\kappa\omega$ we conclude

$$a_l = \int_{-1}^1 \left(\frac{1 - \omega^2}{(1 + \kappa^2 - 2\kappa\omega)} \right)^l \frac{\kappa^l}{(1 + \kappa^2 - 2\kappa\omega)} \, d\omega \leq \int_{-1}^1 \frac{\kappa^l}{(1 + \kappa^2 - 2\kappa\omega)} \, d\omega = \kappa^{l-1} \ln \frac{1 + \kappa}{1 - \kappa}.$$

According to Remark 2.16 the assertion is proved. \square

7 Finally, we give an explicit formula for the double Radon transform of the squared singularity kernel.

Theorem 2.20. Let $\kappa \in (0, 1)$ and $\mathcal{R}K$ be the squared singularity kernel. Then its double Radon transform is given by

$$\mathcal{R}\mathcal{R}K(h_1, r_1; h_2, r_2) = \frac{2\kappa((1 + \kappa)/(1 - \kappa))^{-1}}{(1 - 2\kappa \cos(\omega_h + \omega_r) + \kappa^2)^{1/2} (1 + 2\kappa \cos(\omega_h - \omega_r) + \kappa^2)^{1/2}},$$

where we substituted $\omega_h = \angle h_1 h_2$ and $\omega_r = \angle r_1 r_2$.

11 **Proof.** In order to calculate $\mathcal{R}\mathcal{R}K(h_1, r_1; h_2, r_2)$ for $h_i, r_i \in S^2$ we set for abbreviation $A = \cos(\angle(h_1, h_2)) \cos(\angle(r_1, r_2))$
and $B = \sin(\angle(h_1, h_2)) \sin(\angle(r_1, r_2))$. Since for every fixed $h_1, r_1 \in S^2$ and all $g \in \text{SO}(3)$ the Radon transformed
13 kernel $\mathcal{R}K(h_1, r_1, g)$ depends only on $\langle gh, r \rangle$ we can apply integration formula (2.5) and obtain

$$\begin{aligned} \mathcal{R}\mathcal{R}K(h_1, r_1; h_2, r_2) &= \frac{1}{2\pi} \int_{-\pi}^{\pi} \frac{C}{1 - 2\kappa(A + B \cos(\theta)) + \kappa^2} \, d\theta \\ &= \frac{C}{(1 - 2\kappa(A + B) + \kappa^2)^{1/2} (1 + 2\kappa(A - B) + \kappa^2)^{1/2}}, \end{aligned}$$

15 which gives the desired result. \square

3. The zonal basis function method

17 The zonal basis function method is a widely used method for solving approximation problems based on reproducing
kernel Hilbert spaces. The idea is to formulate the approximation problem as a minimization problem. Using the theory
19 of reproducing kernel Hilbert spaces, the solution of the minimization problem can be identified with the solution of
a system of linear equations. If the zonal basis functions used for approximation are positive definite, the system of
21 linear equations is regular. A characterization of all positive definite functions on $\text{SO}(3)$ is given by Gutzmer (cf. [6]).
However, in our setting of reproducing kernel Hilbert spaces positive definiteness is automatically guaranteed (cf. Eq.
23 (2.7)).

3.1. Approximation of the PDF

25 In this section we will deal with the PDF approximation problem. Let $(P_i, h_i, r_i)_{i=1}^N$ be a set of pole figure intensities
of some unknown ODF $f: \text{SO}(3) \rightarrow \mathbb{R}_+$, i.e., for all $i = 1, \dots, N$ it yields $\mathcal{X}f(h_i, r_i) \approx P_i$. We are looking for a
27 function $\tilde{P}: S^2 \times S^2 \rightarrow \mathbb{R}$ that approximates the data and is an admissible PDF, i.e., there is a function $\tilde{f}: \text{SO}(3) \rightarrow \mathbb{R}$

1 with $\mathcal{X}\tilde{f} = \tilde{P}$. The question how well the function \tilde{f} approximates the true ODF f will be addressed in Section 3.4. It
 3 should be stressed that the approach presented here does not observe the nonnegativity property neither of the PDF nor
 5 of the ODF.

Let us fix $\lambda > 0$ and let some reproducing kernel Hilbert space $\mathcal{H}(B_l, S^2 \times S^2)$ be given with $B_l = 0$ for all odd l
 and with reproducing kernel $K_{S^2 \times S^2}$. We consider the minimization problem

$$J(P) := \frac{1}{N} \sum_{i=1}^N (P(h_i, r_i) - P_i)^2 + \lambda \|P\|_{\mathcal{H}(B_l, S^2 \times S^2)}^2 \rightarrow \min$$

with constraints $P \in \mathcal{H}(B_l, S^2 \times S^2)$ and $\int_{S^2 \times S^2} P(h, r) dh dr = 1$. (3.1)

7 The regularization parameter λ determines the balance between smoothness and fitting the measured data points. In
 terms of the reproducing kernel $K_{S^2 \times S^2}$, the minimization functional can be written as

$$J(P) = \frac{1}{N} \sum_{i=0}^N (\langle P, K_{S^2 \times S^2}(h_i, r_i, \cdot) \rangle_{\mathcal{H}(B_l, S^2 \times S^2)} - P_i)^2 + \lambda \|P\|_{\mathcal{H}(B_l, S^2 \times S^2)}^2.$$

In order to observe the constraint $\int_{S^2 \times S^2} P(h, r) dh dr = 1$ we introduce the normalized kernel $\hat{K}_{S^2 \times S^2} = K_{S^2 \times S^2} - B_0^{-2}$
 by subtracting the integral over the kernel, i.e., the zeroth Fourier coefficient. It is well known (cf. [17, Theorem 1.3.1])
 that a solution \tilde{P} of the minimization problem (3.1) has the representation

$$\tilde{P}(h, r) = 1 + \sum_{i=1}^N c_i \hat{K}_{S^2 \times S^2}(h_i, r_i; h, r) \quad \text{with some } c = (c_i)_{i=1}^N \in \mathbb{R}^N.$$

Let $P = (P_i)_{i=1}^N$, $e = (1, \dots, 1)^t$ and let

$$M = (\hat{K}_{S^2 \times S^2}(h_i, r_i; h_j, r_j))_{i,j=1}^N$$

be the Gram matrix of the minimization problem (3.1). Then the minimization functional can be written as

$$J(c) = \frac{1}{N} \|Mc + e - P\|^2 + \lambda(1 + c^t M c).$$

Since the reproducing kernel $K_{S^2 \times S^2}$ is positive definite the matrix $(1/N)M + \lambda \text{Id}$ is regular for all $\lambda > 0$. Therefore,
 the minimization problem has a unique solution $\tilde{P}(h, r)$ given by

$$c = \left(\frac{1}{N} M + \lambda \text{Id} \right)^{-1} (P - e)$$

and Eq. (3.2). Since $\tilde{P} \in \mathcal{H}(B_l, \text{SO}(3))$ and $B_l = 0$ for l odd there is an even function $\tilde{f}_e \in \mathcal{H}((2l+1)^{-1/2} B_l, \text{SO}(3))$
 such that $\mathcal{X}\tilde{f}_e = \tilde{P}$ (cf. Remark 2.12). Moreover, we obtain this function f_e by applying the inverse Radon transform
 (or equivalently the inverse X-ray transform) to \tilde{P}

$$\tilde{f}_e(g) = 1 + \sum_{i=1}^N c_i \mathcal{R}^{-1} K_{S^2 \times S^2}(h_i, r_i; g).$$

3.2. Approximation of the ODF

As in Section 3.1 we consider a set of pole figure intensities $(P_i, h_i, r_i)_{i=1}^N$. But this time we ask for the ODF, i.e.,
 for a function $\tilde{f}: \text{SO}(3) \rightarrow \mathbb{R}$ satisfying

$$\mathcal{X}f(h_i, r_i) \approx P_i, \quad i = 1, \dots, N.$$

First of all we recall Corollary 2.6 saying that the crystallographic X-ray transform maps all odd generalized spherical
 harmonics to zero. This implies that beside the nonnegativity property there is no chance to determine the odd part of

1 an ODF from its X-ray transform. Therefore, the PDF-to-ODF reconstruction problem on the basis of the pole figure intensities $(P_i, h_i, r_i)_{i=1}^N$ can be split into

- 3 1. Estimation of the even part \tilde{f}_e of the true ODF f such that $\mathcal{X}\tilde{f}_e(h_i, r_i) \approx P_i$ for all $i = 1, \dots, N$.
2. Estimation of the odd part \tilde{f}_o of the true ODF f such that $\tilde{f}_e + \tilde{f}_o \geq 0$.

5 In this paper we will deal only with the first step. For the second step, the reader is referred to e.g., Boehlke [1].

Let $\lambda > 0$. In order to find an estimate of the even part of \tilde{f} we fix an arbitrary reproducing kernel Hilbert space $\mathcal{H}(A_l, \text{SO}(3))$ defined on $\text{SO}(3)$ and consider the minimization problem

$$J(f) := \frac{1}{N} \sum_{i=1}^N (\mathcal{X}f(h_i, r_i) - P_i)^2 + \lambda \|f\|_{\mathcal{H}(A_l, \text{SO}(3))}^2 \rightarrow \min$$

with constraints $f \in \mathcal{H}(A_l, \text{SO}(3))$ and $\int_{\text{SO}(3)} f(g) dg = 1$. (3.7)

9 Let $K_{\text{SO}(3)}$ be the reproducing kernel of $\mathcal{H}(A_l, \text{SO}(3))$ and $\hat{K}_{\text{SO}(3)} = K_{\text{SO}(3)} - A_0^{-2}$ its normalization, i.e., for all $g_0 \in \text{SO}(3)$ the integral $\int_{\text{SO}(3)} \hat{K}_{\text{SO}(3)}(g, g_0) dg$ vanishes. Corollary 2.18 states that for every pair $h, r \in S^2$ the functional $f \mapsto \mathcal{R}f(h_i, r_i)$ is bounded on $\mathcal{H}(A_l, \text{SO}(3))$. Since for every bounded linear functional L on $\mathcal{H}(A_l, \text{SO}(3))$ we have $Lf = \langle f, LK_{\text{SO}(3)} \rangle_{\mathcal{H}(A_l, \text{SO}(3))}$ the minimization functional J can be expressed as

$$J(f) = \frac{1}{N} \sum_{i=0}^N (\langle f, \mathcal{X}K(h_i, r_i, \cdot) \rangle_{\mathcal{H}(A_l, \text{SO}(3))} - P_i)^2 + \lambda \|f\|_{\mathcal{H}(A_l, \text{SO}(3))}^2.$$

As in Section 3.1 we conclude that every solution \tilde{f} of the minimization problem (3.7) has the representation

$$\tilde{f}(g) = 1 + \sum_{i=1}^N c_i \mathcal{X}\hat{K}_{\text{SO}(3)}(h_i, r_i, g) \quad \text{with some } c = (c_i)_{i=1}^N \in \mathbb{R}^N.$$

As a consequence we see that the solution of the minimization problem (3.7) is an even function, i.e., all odd order Fourier coefficients are zero. Let $P = (P_i)_{i=1}^N$, $e = (1, \dots, 1)^t$ and let

$$M = ((\mathcal{X}\hat{K}_{\text{SO}(3)})(h_i, r_i; \cdot), (\mathcal{X}\hat{K}_{\text{SO}(3)})(h_j, r_j; \cdot))_{i,j=1}^N \\ = ((\mathcal{X}\mathcal{X}\hat{K}_{\text{SO}(3)})(h_i, r_i; h_j, r_j))_{i,j=1}^N$$

19 be the Gram matrix of the minimization problem (3.7). Then the penalty functional can be written as

$$J(c) = \frac{1}{N} \|Mc + e - P\|^2 + \lambda(1 + c^t Mc)$$

21 and the solution of the minimization problem is given by

$$c = \left(\frac{1}{N} M + \lambda \text{Id} \right)^{-1} (P - e)$$

23 and Eq. (3.6).

Comparing the definitions (3.3) and (3.8) for the Gram matrices we see that for $K_{S^2 \times S^2} = \mathcal{X}\mathcal{X}K_{\text{SO}(3)}$ both minimization problems (3.1) and (3.7) lead to the same system of linear equations (3.4) and (3.9) and therefore have the same solution $\tilde{f}_e = \tilde{f}$. However, in the minimization problem (3.1) we claimed just that $\mathcal{H}(B_l, S^2 \times S^2)$ is a reproducing

1 kernel Hilbert space, i.e., $\sum_{l \in \mathbb{N}(B)} (2l+1)^2/B_l^2 < \infty$, whereas in the minimization problem (3.7) we claimed that
 2 $\mathcal{H}(A_l, \text{SO}(3))$ is a reproducing kernel Hilbert space, i.e., $\sum_{l \in \mathbb{N}(A)} (2l+1)^2/A_l^2 = \sum_{l \in \mathbb{N}(B)} (2l+1)^3/B_l^2 < \infty$.

3 3.3. Crystal symmetries

4 So far we have not considered crystal symmetries at all. However, they are not only necessary to obtain correct
 5 results, but also improve the accuracy of the calculation.

6 Let $G \subseteq \text{SO}(3)$ be the point group of a crystal and $\mathcal{H}(A_l, \text{SO}(3))$, $\mathcal{H}(B_l, S^2 \times S^2)$ two reproducing kernel Hilbert
 7 spaces as defined in Section 2.4 such that $\mathcal{R}\mathcal{H}(A_l, \text{SO}(3)) = \mathcal{H}(B_l, S^2 \times S^2)$. For both we define the symmetrization
 8 operator

$$9 \quad \begin{aligned} S_G: \mathcal{H}(\text{SO}(3)) &\rightarrow \mathcal{H}(\text{SO}(3)) \quad \text{and} \quad S_G: \mathcal{H}(S^2 \times S^2) \rightarrow \mathcal{H}(S^2 \times S^2), \\ S_G f(g) &= \sum_{g_S \in G} f(gg_S), \quad S_G P(h, r) = \sum_{g_S \in G} P(g_S h, r) \end{aligned}$$

10 and denote its image by $\mathcal{H}_G(\text{SO}(3))$ and $\mathcal{H}_G(S^2 \times S^2)$, respectively. Let $K_{\text{SO}(3)}$ and $K_{S^2 \times S^2}$ be the reproducing
 11 kernels of $\mathcal{H}(\text{SO}(3))$ and $\mathcal{H}(S^2 \times S^2)$. It is easy to see that $\mathcal{H}_G(\text{SO}(3))$ and $\mathcal{H}_G(S^2 \times S^2)$ are reproducing kernel
 12 Hilbert spaces and their reproducing kernels are given by $S_G K_{\text{SO}(3)}$ and $S_G K_{S^2 \times S^2}$. The calculation

$$13 \quad \begin{aligned} (\mathcal{R}f(\cdot g_S^{-1}))(h, r) &= \int_{\{g \in \text{SO}(3) \mid gh=r\}} f(gg_S^{-1}) dg \\ &= \int_{\{g' \in \text{SO}(3) \mid g'g_S h=r\}} f(g') dg' = (\mathcal{R}f)(g_S h, r) \end{aligned}$$

14 shows that S_G commutes with the Radon transform. Hence, there exists a restriction \mathcal{R}_G of \mathcal{R} to $\mathcal{H}_G(\text{SO}(3))$ and
 15 $\mathcal{H}_G(S^2 \times S^2)$. In particular, the diagram

$$\begin{array}{ccc} \mathcal{H}(\text{SO}(3)) & \xrightarrow{\mathcal{R}} & \mathcal{H}(S^2 \times S^2) \\ \downarrow S_G & & \downarrow S_G \\ \mathcal{H}_G(\text{SO}(3)) & \xrightarrow{\mathcal{R}_G} & \mathcal{H}_G(S^2 \times S^2) \end{array}$$

16 commutes. It is straightforward to check that we can apply the zonal basis function method from Sections 3.1 and 3.2
 17 to the PDF and ODF reconstruction problem involving the crystal symmetry G just by replacing $K_{\text{SO}(3)}$ by $S_G K_{\text{SO}(3)}$
 18 and $K_{S^2 \times S^2}$ by $S_G K_{S^2 \times S^2}$.

3.4. Error estimates

19 Let throughout this section $(P_i, h_i, r_i)_{i=1}^N$ be a set of pole figure data. Let furthermore $\mathcal{H}(A_l, \text{SO}(3))$ and $\mathcal{H}(B_l, S^2 \times S^2)$
 20 be two reproducing kernel Hilbert spaces with reproducing kernels $K_{S^2 \times S^2}$ and $K_{\text{SO}(3)}$ such that $\mathcal{R}\mathcal{H}(A_l, \text{SO}(3)) =$
 21 $\mathcal{H}(B_l, S^2 \times S^2)$. For every pair of directions $(h', r') \in S^2 \times S^2$, the proximity to the data points can be described by

$$22 \quad C(h', r') = \min_{i=1, \dots, N} (K_{S^2 \times S^2}(0, 0) - K_{S^2 \times S^2}(\angle h' h_i, \angle r' r_i)). \quad (3.10)$$

23 Suppose f is the true ODF and P the true PDF of the specimen. Here, we want to perform an error estimate for the
 24 reconstructed PDF \hat{P} and the reconstructed even part of the ODF \hat{f}_e , obtained as solutions of the minimization problems
 25 (3.1) and (3.7).

26 It is quite natural that we have to postulate additional properties for the true ODF in order to get error bounds.
 27 Following the general framework of interpolation in reproducing kernel Hilbert spaces (cf. [5, Theorem 6.2.1]) we can
 28 prove the following theorem claiming the ODF to have a bounded Sobolev norm.

29 **Theorem 3.1.** *Let $f \in \mathcal{H}(A_l, \text{SO}(3))$ be the ODF of a specimen, $P \in \mathcal{H}(B_l, S^2 \times S^2)$ the corresponding PDF
 30 and $(P_i, h_i, r_i)_{i=1}^N$ a set of pole figure intensities. Denote by \hat{P} the solution of the minimization problem 3.1 and*

1 by $\varepsilon = \max_{i=1,\dots,N} \|\tilde{P}(h_i, r_i) - P_i\|$ the approximation error in the data points. Then for every pair of directions
 (h', r') $\in S^2 \times S^2$ we have

$$|P(h', r') - \tilde{P}(h', r')|^2 \leq \max_{i=1,\dots,N} \varepsilon_i^2 + 2C(h', r') \|P\|_{\mathcal{H}(B_l, S^2 \times S^2)}^2$$

$$\leq \varepsilon^2 + 2C(h', r') \|f\|_{\mathcal{H}(A_l, \text{SO}(3))}^2, \quad (3.11)$$

where $C(h', r')$ is defined as in Eq. (3.10).

5 **Proof.** For every $i = 1, \dots, N$, the triangle inequality yields

$$|\tilde{P}(h', r') - P(h', r')| \leq |\tilde{P}(h', r') - \tilde{P}(h_i, r_i)| + |\tilde{P}(h_i, r_i) - P(h_i, r_i)| + |P(h_i, r_i) - P(h', r')|.$$

7 Writing

$$\tilde{P}(h', r') - \tilde{P}(h_i, r_i) = \langle K(h', r'; \cdot) - K(h_i, r_i; \cdot), \tilde{P} \rangle_{\mathcal{H}(B_l, S^2 \times S^2)},$$

$$P(h', r') - P(h_i, r_i) = \langle K(h', r'; \cdot) - K(h_i, r_i; \cdot), P \rangle_{\mathcal{H}(B_l, S^2 \times S^2)}$$

9 we obtain by the Cauchy–Schwarz inequality

$$|\tilde{P}(h', r') - \tilde{P}(h_i, r_i)| \leq \|K(h', r'; \cdot) - K(h_i, r_i; \cdot)\|_{\mathcal{H}(B_l, S^2 \times S^2)} \|\tilde{P}\|_{\mathcal{H}(B_l, S^2 \times S^2)},$$

$$|P(h', r') - P(h_i, r_i)| \leq \|K(h', r'; \cdot) - K(h_i, r_i; \cdot)\|_{\mathcal{H}(B_l, S^2 \times S^2)} \|P\|_{\mathcal{H}(B_l, S^2 \times S^2)}.$$

11 For the first norm in the product we obtain the estimate

$$\langle K(h', r'; \cdot) - K(h_i, r_i; \cdot), K(h', r'; \cdot) - K(h_i, r_i; \cdot) \rangle_{\mathcal{H}(B_l, S^2 \times S^2)}$$

$$= K(h', r'; h', r') + K(h_i, r_i; h_i, r_i) - 2K(h_i, r_i; h', r')$$

$$= 2(K(0, 0) - K(\angle h'h; \angle r'r))$$

$$= 2C(h', r').$$

13 Since \tilde{P} is the smoothest approximation of the data its Sobolev norm is bounded by $\|\tilde{P}\|_{\mathcal{H}(B_l, S^2 \times S^2)} \leq \|P\|_{\mathcal{H}(B_l, S^2 \times S^2)} \leq \|f\|_{\mathcal{H}(A_l, \text{SO}(3))}$ and Eq. (3.11) follows. \square

15 **Remark 3.2.** Let G be a point group and S_G the symmetrization operator as defined in Section 3.3. Let further \tilde{P} be
 the solution of the interpolation problem (3.1) with respect to the symmetrized kernel $S_G K_{S^2 \times S^2}$. Then Theorem 3.1
 17 remains valid if we replace for all $h', r' \in S^2$ the factor $C(h', h')$ by the symmetrized version

$$C_G(h', r') = \min_{h \in Gh'} C(h, r'). \quad (3.12)$$

19 Defining

$$C_N = \max_{r, h \in S^2} C_G(h, r) \quad (3.13)$$

21 we obtain a measure of the tightness of the data points relatively to the reproducing kernel Hilbert space $\mathcal{H}(B_l, S^2 \times S^2)$.
 With this constant equation, (3.11) rewrites as

$$\|P - \tilde{P}\|_{\infty}^2 \leq \varepsilon^2 + 2C_N \|f\|_{\mathcal{H}(A_l, \text{SO}(3))}^2. \quad (3.14)$$

The Sobolev norm of an ODF \tilde{f} can be interpreted as follows. Let f be the true ODF of a specimen with texture
 25 index $\|f\|_{L^2(\text{SO}(3))}^2 = \int_{\text{SO}(3)} |f(g)|^2 dg$. Then the Sobolev norm of the convolution with the reproducing kernel yields
 $\|f * K(\text{Id}, \cdot)\|_{\mathcal{H}(A_l, \text{SO}(3))} = \|f\|_{L^2(\text{SO}(3))}$. On the other hand, the measurement of a PDF always involves a smoothing
 27 process, i.e., a convolution with a kernel function. That means we do not reconstruct the true PDF or ODF but a
 smoothed version of it and the Sobolev norm of the smoothed ODF is given by the texture index of the true ODF.

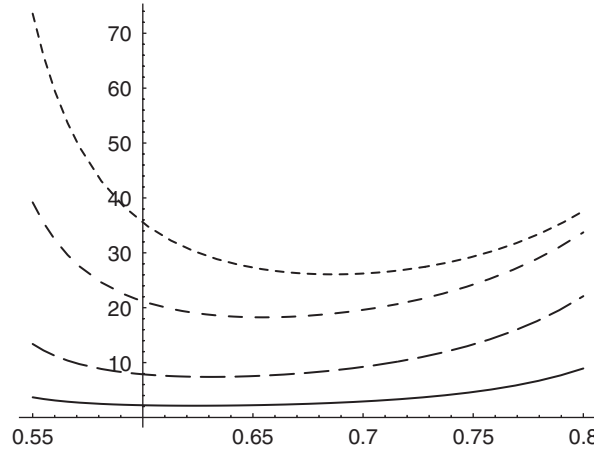


Fig. 2. The error bounds $C_N \|f\|_{\mathcal{H}(A_l, \text{SO}(3))}^2$ corresponding to the Sobolev space $\mathcal{H}((2l+1)/2\pi)\kappa^l$, $\text{SO}(3)$ as a function in κ for a fixed ODF and proximity coefficients $\Delta h \in \{\pi/4, \pi/8, \pi/16, \pi/32\}$ (from top to bottom).

1 In order to investigate the dependence of the error estimate from the kernel function we consider the unimodal
 distributed ODF $f(g) = (1 - \chi^2)/(1 - 2\chi \cos(\angle g) + \chi^2)^{3/2}$ with $\chi = 0.7$. In Fig. 2 the error bound $C_N \|f\|_{\mathcal{H}(A_l, \text{SO}(3))}^2$
 3 corresponding to the Sobolev space $\mathcal{H}(A_l, \text{SO}(3))$ with coefficients $A_l = ((2l+1)/2\pi)\kappa^l$ is plotted as a function of κ
 and for proximity coefficients $\Delta h \in \{\pi/4, \pi/8, \pi/16, \pi/32\}$.

5 In the next theorem we prove an error bound for the reconstructed even part \tilde{f}_e of the ODF f .

Theorem 3.3. Let $f_e \in \mathcal{H}(A_l, \text{SO}(3))$ be the even part of an ODF, $P \in \mathcal{H}(B_l, S^2 \times S^2)$ the corresponding PDF and
 7 $(P_i, r_i, h_i)_{i=1}^N$ a set of pole figure intensities. Denote by C_N the constant defined in Eq. (3.13), by \tilde{f}_e the solution of the
 minimization problem 3.7 and by $\varepsilon_i = |\mathcal{X}\tilde{f}_e(h_i, r_i) - P_i|$ the approximation error in the data points. Then we have

$$9 \quad \|f_e - \tilde{f}_e\|_{\mathcal{H}(A_l^{1/2}, \text{SO}(3))} \leq 2(\varepsilon^2 + 2C_N \|f\|_{\mathcal{H}(A_l, \text{SO}(3))}^2)^{1/2} \|f\|_{\mathcal{H}(A_l, \text{SO}(3))}. \quad (3.15)$$

Proof. For an even function $\phi \in \mathcal{H}(A_l, \text{SO}(3))$ and $\Phi = \mathcal{X}\phi \in \mathcal{H}(B_l, S^2 \times S^2)$ we compute

$$\begin{aligned} \|\phi\|_{\mathcal{H}(A_l^{1/2}, \text{SO}(3))}^2 &= \|\Phi\|_{\mathcal{H}(B_l^{1/2}, S^2 \times S^2)}^2 \\ &= \sum_{l=0}^{\infty} \sum_{i,j=-l}^l B_l |\hat{\Phi}(l, i, j)|^2 \\ &\leq \left(\sum_{l=0}^{\infty} \sum_{i,j=-l}^l |\hat{\Phi}(l, i, j)|^2 \right) \left(\sum_{l=0}^{\infty} \sum_{i,j=-l}^l B_l^2 |\hat{\Phi}(l, i, j)|^2 \right) \\ 11 \quad &\leq \|\Phi\|_{L^2(S^2 \times S^2)}^2 \|\Phi\|_{\mathcal{H}(B_l, S^2 \times S^2)}^2 \leq \|\mathcal{X}\phi\|_{\infty}^2 \|\phi\|_{\mathcal{H}(A_l, \text{SO}(3))}^2. \end{aligned}$$

13 Setting $\phi = f_e - \tilde{f}_e$ and applying Eq. (3.14) to $\|\mathcal{X}\phi\|_{\infty}$ we obtain the first part of the assertion. Since \tilde{f}_e is the solution
 of the minimization problem (3.7) we finish with $\|f_e - \tilde{f}_e\|_{\mathcal{H}(A_l, \text{SO}(3))} \leq 2\|f_e\|_{\mathcal{H}(A_l, \text{SO}(3))} \leq 2\|f\|_{\mathcal{H}(A_l, \text{SO}(3))}$. \square

15 **Remark 3.4.** If additionally to Theorem 3.3 the space $\mathcal{H}(A_l^{1/2}, \text{SO}(3))$ is a reproducing kernel Hilbert space then
 there is a constant $C > 0$ such that $\|g\|_{\infty} \leq C\|f\|_{\mathcal{H}(A_l^{1/2}, \text{SO}(3))}$. In particular, it follows that every even ODF f can be
 approximated arbitrary well, at least if the data are sufficiently dense on $S^2 \times S^2$.

Table 1

The relative errors of the estimated PDF and ODF to f with respect to the squared singularity kernel with $\kappa = 0.7$ and different sets of X-ray intensities

X-ray intensities	$\frac{\ P - \tilde{P}\ _\infty}{\ P\ _\infty}$	$\frac{\ f_e - \tilde{f}_e\ _\infty}{\ f_e\ _\infty}$	$\frac{\ f - \tilde{f}\ _\infty}{\ f\ _\infty}$
5×74	0.12	0.17	0.22
5×180	0.04	0.11	0.16
5×390	0.04	0.08	0.13
5×770	0.04	0.03	0.07

4. Numerical results

In this section we present numerical results we obtained applying the zonal basis function method to generate pole figure intensities. The de la Vallée Poussin kernel is defined by

$$K = \frac{B(3/2, 1/2)}{B(3/2, \kappa + 1/2)} \cos^{2\kappa} \frac{\omega}{2},$$

where the parameter κ describes the concentration of K . As a test ODF we choose the superposition of two de la Vallée Poussin-shaped components with an uniformly distributed background

$$\tilde{f}(g) = 0.3 + \sum_{i=1}^2 \lambda_i K(g_i, g),$$

where the first component is centred in $g_1 = \text{Id}$ and has the parameter $\kappa_1 = 15$ and the second component has centre in $g_2 = (0, 10, 0)$ (Euler angles) and parameter $\kappa_2 = 76$. The coefficients are set to $\lambda_1 = 0.6$ and $\lambda_2 = 0.1$. Hence, the ODF \tilde{f} is nearly unimodal distributed with none radial symmetric peak in the identical rotation. Finally, we obtain a cubic symmetric ODF

$$f(g) = \sum_{\hat{g} \in T} \tilde{f}(g\hat{g})$$

by summation of \tilde{f} over the cubical point group T . Using the fact that

$$(\mathcal{R}K)(g, h, r) = (1 + \kappa) \cos^{2\kappa} \frac{\angle(gh, r)}{2}$$

the PDF of f can be easily calculated. In order to simulate an X-ray diffraction experiment, we calculate the pole figures to the crystal directions $(1, 0, 0)$, $(1, 1, 0)$, $(1, 1, 1)$, $(2, 1, 1)$ and $(2, 2, 1)$ and a set of approximately equidistant distributed specimen directions and add to them some $\mathcal{N}(0, 0.05^2)$ -distributed noise. In Table 1 the relationship between the number of X-ray intensities and the relative error is presented. In all cases we used the regularization parameter $\lambda = 1$.

5. Conclusions and outlook

We presented a method that allows to reconstruct the PDF and the even part of an ODF from a set of X-ray intensities by superposition of fibre ODFs and corresponding PDFs, respectively. The advantage of the method is that it can deal with X-ray intensities of arbitrary arranged crystal and specimen directions. Moreover, the solution is adapted to this arrangement in the sense that in regions where the crystal and specimen directions are dense the solution is effected by many kernel functions and therefore approximates more exactly than in regions of coarser measurements.

A second advantage of the zonal basis function method is the simple numerical implementation. The problem reduces to solve a system of linear equations where the matrix is symmetric positive definite. In the special case that the grid (h_i, r_i) provides for each h a regular structure on S^2 the matrix turns out to be of block Toeplitz structure.

1 A disadvantage of the presented method is that it does not consider the nonnegativity property of the PDF. However,
the general approximation theorem of the zonal basis function method implies that the negative minimum of the
3 estimated PDF is bounded by a constant which converges to the true minimum if more X-ray intensities are measured.

Acknowledgements

The authors J.P., H.S. and R.H. gratefully acknowledge funding by Deutsche Forschungsgemeinschaft Grant SCHA 465/15 and PR 331/11.

5 References

- 7 [1] T. Boehlke, Application of the maximum entropy method to texture analysis, submitted for publication.
[2] H.J. Bunge, *Mathematische Methoden der Texturanalyse*, Akademie Verlag, Berlin, 1969.
9 [3] W. Cheney, W. Light, *A Course in Approximation Theory*, Brookes/Cole, Pacific Groove, CA, 1999.
[4] D.L. Donoho, Orthonormal ridgelets and linear singularities, *SIAM J. Math. Anal.* 31 (2000) 1062–1099.
[5] W. Freeden, T. Gervens, M. Schreiner, *Constructive Approximation on the Sphere*, Clarendon Press, Oxford, 1998.
11 [6] T. Gutzmer, Interpolation by positive definite functions on locally compact groups with applications to $SO(3)$, *Result. Math.* 29 (1996) 69–77.
[7] S. Helgason, *The Radon Transform*, second ed., Birkhäuser, Basel, 1999.
13 [8] K. Helming, Th. Eschner, A new approach to texture analysis of multiphase materials using a texture component model, *Cryst. Res. Technol.* 25 (1990) K203–K208.
15 [9] S. Hubbert, Radial basis function interpolation on the sphere, Dissertation, Imperial College, London, 2002.
[10] S. Matthies, G.W. Vinel, K. Helmig, Standard Distributions in Texture Analysis, Akademie-Verlag, Berlin, 1987.
17 [11] L. Meister, H. Schaeben, A concise quaternion geometry of rotations, *MMAS* 28 (2004) 101–126.
[12] C. Müller, *Spherical Harmonics*, Springer, Berlin, 1966.
19 [13] H. Schaeben, *Diskrete mathematische Methoden zur Berechnung und Interpretation von kristallographischen Orientierungsdichten*, DGM Informationsgesellschaft Verlag, 1994.
21 [14] H. Schaeben, A simple standard orientation density function: the hyperspherical de la Vallée Poussin kernel, *Phys. Stat. Sol. B* 200 (1997) 367–376.
23 [15] D. Schwarzenbach, *Kristallographie*, Springer, Berlin, 2001.
[16] N.Ja. Vilenkin, A.U. Klimyk, *Representation of Lie Groups and Special Functions*, vol. 1, Kluwer Academic Publishers, Dordrecht, 1991.
25 [17] G. Wahba, *Spline models for observational data*, CBMS-NFS Regional Conference Series in Applied Mathematics, vol. 59, SIAM, Philadelphia, PA, 1990.